

IMECE2011-63179

**FINITE DEFORMATION ELASTOPLASTICITY FOR RATE AND TEMPERATURE
 DEPENDENT POLYCRYSTALLINE METALS**

Richard A. Regueiro*

Department of Civil, Environmental,
 and Architectural Engineering
 University of Colorado at Boulder
 428 UCB
 Boulder, Colorado, 80309
 Email: regueiro@colorado.edu

Douglas J. Bammann

Esteban B. Marin
 Center for Advanced Vehicular Systems
 Mississippi State University
 MS 1740
 Mississippi State, Mississippi, 39762
 Email: bammann@cavs.msstate.edu,
 ebmarin@cavs.msstate.edu

George C. Johnson

Department of Mechanical Engineering
 University of California, Berkeley
 MS 1740
 Berkeley, California, 94720
 Email: gjohnson@me.berkeley.edu

ABSTRACT

An elastoplasticity model is formulated and demonstrated in one-dimension (1D) for modeling finite deformations in polycrystalline metals. Quasi-static to high strain rate effects as well as temperature sensitivity are included. A multiplicative decomposition of the deformation gradient into elastic, plastic, and thermal parts, that includes a volumetric/isochoric split of the elastic stretching tensor is assumed. The kinematics and thermodynamic formulation lead to constitutive equations, stresses, and constraints on the evolution of the internal state variables. The model accounts for (i) dislocation drag effects on flow stress, and (ii) generation (hardening) and annihilation (recovery) of statistically-stored dislocations (SSDs). The resulting model is normalized to dimensionless form to allow dimensionless material parameters fit for one metal to approximate the behavior of another metal of similar lattice structure, if data are limited. One dimensional material parameter fitting is demonstrated for two refractory metals, body centered cubic (bcc) Tantalum and Tungsten.

NOTATION

Boldface denotes vectors and tensors in symbolic notation. Unless otherwise indicated, all vector and tensor products in symbolic form are assumed to be inner products, such as $\boldsymbol{v}\boldsymbol{v} =$

$v_i v_i$, $(\boldsymbol{a}\boldsymbol{b})_{ik} = a_{ij}b_{jk}$, and $\boldsymbol{a} : \boldsymbol{b} = a_{ij}b_{ij}$, where repeated indices denote a sum over those indices. The symbol $:=$ denotes a definition. An overbar ($\bar{\bullet}$) designates a variable in the intermediate configuration $\bar{\mathcal{B}}$, and different symbols for the other intermediate configurations. Uppercase letters are for the most part reserved for variables in the reference and intermediate configurations, and lowercase letters for the most part designate variables in the current configuration. Cartesian coordinates are assumed. This convention applies to indices as well: S_{IJ} is in the reference configuration \mathcal{B}_0 , $\bar{S}_{\bar{I}\bar{J}}$ in the intermediate configuration $\bar{\mathcal{B}}$, and σ_{ij} in the current configuration \mathcal{B} . The symbol $\text{tr}(\bullet)$ is the trace operator, such that $\text{tr}(\boldsymbol{\sigma}) = \sigma_{ii}$. The symbol $\text{dev}(\bullet)$ is the deviatoric operator, such that $\text{dev}(\boldsymbol{\sigma}) = \boldsymbol{\sigma} - \frac{1}{3}(\text{tr}\boldsymbol{\sigma})\mathbf{1}$. The accent symbol $\acute{\bullet}$ denotes an isochoric elastic deformation measure. The symbol $\text{sym}(\bullet)$ denotes the symmetric part of a second order tensor, such that $\text{sym}(\boldsymbol{\ell}) = (\boldsymbol{\ell} + \boldsymbol{\ell}^T)/2$, and $\text{skw}(\bullet)$ the skew-symmetric part of the tensor, such that $\text{skw}(\boldsymbol{\ell}) = (\boldsymbol{\ell} - \boldsymbol{\ell}^T)/2$. The symbol $(\bullet)^T$ denotes transpose of a tensor. The symbol $\dot{\bullet}$ is the material time derivative. The symbol $\|\bullet\|$ is the L_2 norm of a vector or tensor, such that $\|\boldsymbol{a}\| = \sqrt{a_{ij}a_{ij}}$. The symbol $\mathbf{1}$ is the unity tensor, i.e., $(\mathbf{1})_{ij} = \delta_{ij}$, where δ_{ij} is the Kronecker delta. The symbol $(\overset{\circ}{\bullet})$ over a variable denotes that it is dimensionless.

*Address all correspondence to this author.

INTRODUCTION

Polycrystalline metals that undergo high strain rates—possibly nearing the shock regime ($> 10^4$ 1/s)—experience a complex combination of deformation mechanisms, such as thermally-activated dislocation motion and generation, dislocation annihilation, dislocation drag, texture effects, recrystallization and grain growth, void nucleation, growth, and coalescence, infinitesimal isochoric elastic stretching, potentially large volumetric elastic stretching, and large rotations, for instance. The elastoplasticity model described in this paper is a phenomenological description of the physical deformation mechanisms observed at the dislocation length scale in polycrystalline metals. In the literature, more complex constitutive models have been developed that include spatial gradients of internal state variables [1–3] and free surface creation due to crack propagation [4], among other deformation mechanisms and material processes experienced by polycrystalline metals (e.g., recrystallization and grain growth, phase transformations). We limit the model described in this paper to temperature and rate-dependent isotropic elastoplasticity. Damage and texture effects will be considered in future papers.

The formulation of the model begins with a description of the kinematics, through a multiplicative decomposition of the deformation gradient. We formulate the constitutive equations in the plastically deformed, elastically unloaded, intermediate configuration $\tilde{\mathcal{B}}$. Constitutive assumptions are made for the Helmholtz free energy density reflecting infinitesimal isochoric elastic deformations in polycrystalline metals, but potentially large volumetric elastic deformation for an initially undamaged metal loaded in the near shock strain-rate regime. A dimensionless form of the model is presented in the current configuration, and material parameter fitting for this dimensionless form is demonstrated for two metals of similar lattice structure (body centered cubic (bcc) Tantalum and Tungsten).

MODEL FORMULATION

The formulation of a thermodynamically-consistent, finite strain, elastoplastic constitutive model for solids, in this case for a polycrystalline metal, proceeds in the following order: (i) kinematics, (ii) thermodynamics, and (iii) constitutive equations with parameter fitting.

Kinematics

For finite deformation elastoplastic constitutive modeling, we assume a multiplicative decomposition of the deformation gradient as [5–8]

$$\mathbf{F} = \mathbf{F}^e \mathbf{F}^p \mathbf{F}^\theta, \quad F_{iI} = F_{i\tilde{I}}^e F_{\tilde{I}\bar{I}}^p F_{\bar{I}I}^\theta \quad (1)$$

where e stands for elastic, p for plastic, and θ for the temperature part of \mathbf{F} (Fig.1). The order of decomposition is not arbitrary. The first map \mathbf{F}^θ implies that there can be deformation due to temperature change (thermal expansion) without elastic or plastic deformation, where the plastic deformation for polycrystalline metals we consider to be primarily thermally-activated dislocation motion (although dislocation drag at high rates can occur). Macroscopic elastic deformation through \mathbf{F}^e can be unloaded from the current configuration \mathcal{B} to the intermediate configuration $\tilde{\mathcal{B}}$. The intermediate configuration (plastically deformed) $\tilde{\mathcal{B}}$ is a physically obtainable configuration by unloading elastically.

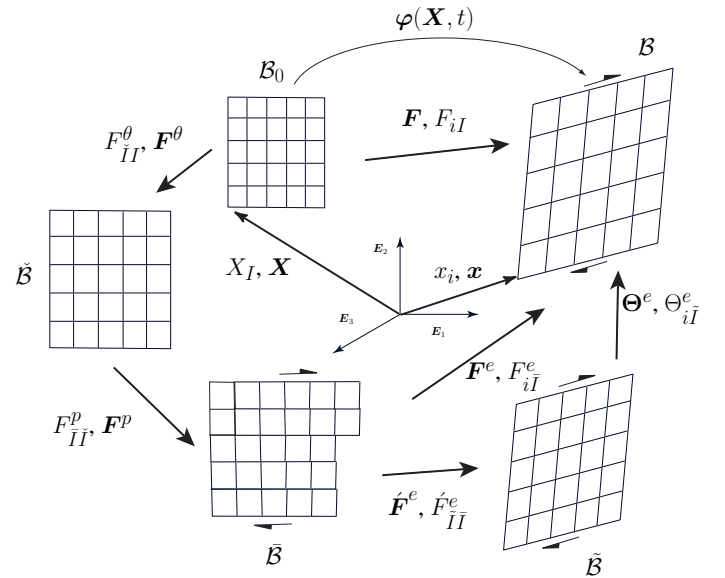


FIGURE 1. Multiplicative decomposition of the deformation gradient $\mathbf{F} = \Theta^e \tilde{\mathbf{F}}^e \mathbf{F}^p \mathbf{F}^\theta$, $F_{iI} = \Theta_{i\tilde{I}}^e \tilde{F}_{\tilde{I}\bar{I}}^e F_{\bar{I}I}^p F_{\bar{I}I}^\theta$. Note that $\tilde{\mathcal{B}}$ is an incompatible configuration, but for the purpose of phenomenological elastoplasticity modeling, the mapping \mathbf{F}^p will be treated as a smooth mapping (i.e., no jump discontinuities or free surfaces at the dislocation scale are considered).

One of two polar decompositions of the elastic part of the deformation gradient \mathbf{F}^e is $\mathbf{F}^e = \mathbf{V}^e \mathbf{R}^e$ ($F_{i\tilde{I}}^e = V_{i\tilde{I}}^e R_{\tilde{I}\bar{I}}^e$), where \mathbf{V}^e is an elastic stretching tensor and \mathbf{R}^e is an elastic proper orthogonal tensor (cf. [9] for more discussion of these and other finite deformation plasticity kinematics). The elastic stretch tensor may be split into volumetric and isochoric parts as [10, 11]

$$\mathbf{V}^e = \Theta^e \tilde{\mathbf{V}}^e, \quad V_{i\tilde{I}}^e = \Theta_{i\tilde{I}}^e \tilde{V}_{\tilde{I}\bar{I}}^e \quad (2)$$

$$\Theta_{i\tilde{I}}^e = (J^e)^{1/3} \delta_{i\tilde{I}}, \quad \det \Theta^e = J^e = \det \mathbf{V}^e \quad (3)$$

$$\tilde{V}_{\tilde{I}\bar{I}}^e = (J^e)^{-1/3} \delta_{\tilde{I}\bar{I}} V_{a\bar{I}}^e, \quad \det \tilde{\mathbf{V}}^e = 1 \quad (4)$$

and then the elastic part of the deformation gradient is written as

$$\mathbf{F}^e = \Theta^e \tilde{\mathbf{V}}^e \mathbf{R}^e = \Theta^e \dot{\mathbf{F}}^e \quad (5)$$

$$F_{i\bar{I}}^e = \Theta_{i\bar{I}}^e \tilde{V}_{i\bar{I}}^e R_{j\bar{I}}^e = \Theta_{i\bar{I}}^e \dot{F}_{i\bar{I}}^e = (J^e)^{1/3} \delta_{i\bar{I}} \dot{F}_{i\bar{I}}^e = (J^e)^{1/3} \dot{F}_{i\bar{I}}^e$$

The volumetric/isochoric split is appropriate for modeling metals that experience strain rates within the shock regime ($> 10^4$ 1/s), where pressure and volumetric elastic deformation can be large for an initially undamaged metal [6]. The isotropic volumetric deformation due to change in temperature θ is written as

$$F_{i\bar{I}}^\theta := F^\theta(\theta) \delta_{i\bar{I}} = (J^\theta)^{1/3} \delta_{i\bar{I}}, \quad J^\theta = \det \mathbf{F}^\theta = [F^\theta(\theta)]^3 \quad (6)$$

where $F^\theta(\theta)$ is a function of temperature θ . The multiplicative decomposition then becomes

$$\begin{aligned} \mathbf{F} &= \Theta^e \dot{\mathbf{F}}^e \mathbf{F}^p \mathbf{F}^\theta, \quad F_{i\bar{I}} = \Theta_{i\bar{I}}^e \dot{F}_{i\bar{I}}^e F_{i\bar{I}}^p F_{i\bar{I}}^\theta \\ &= (J^e J^\theta)^{1/3} \dot{\mathbf{F}}^e \mathbf{F}^p, \quad F_{i\bar{I}} = (J^e J^\theta)^{1/3} \dot{F}_{i\bar{I}}^e F_{i\bar{I}}^p \end{aligned} \quad (7)$$

where $F_{i\bar{I}}^p = F_{i\bar{I}}^p \delta_{i\bar{I}}$. When writing the left and right isochoric elastic Cauchy-Green tensors, the index forms $\dot{F}_{i\bar{I}}^e$ and $\dot{F}_{i\bar{I}}^e$ will be used equivalently, given that configurations \mathcal{B} and $\bar{\mathcal{B}}$ map through an isotropic tensor, Θ^e (cf. Fig.1). We write the right isochoric elastic Cauchy-Green tensor as $\dot{\mathbf{C}}^e = (\dot{\mathbf{F}}^e)^T \dot{\mathbf{F}}^e$, where $\dot{C}_{i\bar{I}j\bar{I}}^e = \dot{F}_{i\bar{I}}^e \dot{F}_{j\bar{I}}^e$, with isochoric elastic Lagrangian strain $\dot{\mathbf{E}}^e = (\dot{\mathbf{C}}^e - \bar{\mathbf{1}})/2$. Likewise, we write the left isochoric elastic Cauchy-Green tensor as $\dot{\mathbf{b}}^e = \dot{\mathbf{F}}^e (\dot{\mathbf{F}}^e)^T$, where $\dot{b}_{ij}^e = \dot{F}_{i\bar{I}}^e \dot{F}_{j\bar{I}}^e$. Note that the Jacobian of deformation becomes $J = \det \mathbf{F} = J^e J^\theta$, where plastic deformation (dislocation motion) is isochoric for metals, such that $J^p = \det \mathbf{F}^p = 1$. The velocity gradient in the current configuration \mathcal{B} then takes the form

$$\begin{aligned} \boldsymbol{\ell} &= \dot{\mathbf{F}} \mathbf{F}^{-1} \\ &= \underbrace{\frac{j^e}{3J^e} \mathbf{1}}_{\boldsymbol{\ell}^{\Theta^e}} + \underbrace{\dot{\mathbf{F}}^e (\dot{\mathbf{F}}^e)^{-1}}_{\dot{\boldsymbol{\ell}}^e} + \underbrace{\dot{\mathbf{F}}^e \bar{\mathbf{L}}^p (\dot{\mathbf{F}}^e)^{-1}}_{\boldsymbol{\ell}^p} + \underbrace{\frac{\dot{F}^\theta(\theta)}{F^\theta(\theta)} \mathbf{1}}_{\boldsymbol{\ell}^\theta} \end{aligned} \quad (8)$$

where $j^e = J^e (\mathbf{b}^e)^{-1} : \dot{\mathbf{b}}^e/2$, $\mathbf{b}^e = \mathbf{F}^e (\mathbf{F}^e)^T = (J^e)^{2/3} \dot{\mathbf{F}}^e (\dot{\mathbf{F}}^e)^T$, and $\bar{\mathbf{L}}^p = \dot{\mathbf{F}}^p (\mathbf{F}^p)^{-1}$. The symmetric and skew-symmetric parts of the velocity gradient are the deformation rate $\mathbf{d} := \text{sym}(\boldsymbol{\ell})$ and spin $\mathbf{w} := \text{skw}(\boldsymbol{\ell})$.

Thermodynamics

The Clausius-Duhem inequality may be written pointwise in the current configuration \mathcal{B} as

$$\boldsymbol{\sigma} : \boldsymbol{\ell} - \rho \dot{\psi} - \rho \eta \dot{\theta} + \frac{1}{\theta} \mathbf{q} \cdot \nabla \theta \geq 0 \quad (9)$$

and pointwise in the intermediate configuration $\bar{\mathcal{B}}$ as

$$J^e \boldsymbol{\sigma} : \boldsymbol{\ell} - \bar{\rho} \dot{\psi} - \bar{\rho} \eta \dot{\theta} + \frac{1}{\theta} \bar{\mathbf{Q}}(\bar{\nabla} \theta) \geq 0 \quad (10)$$

where $\boldsymbol{\sigma}$ is the symmetric Cauchy stress for a non-polar solid, ρ is the mass density for a single phase solid in \mathcal{B} , $\bar{\rho} = J^e \rho$, ψ is the Helmholtz free energy per unit mass, η is the entropy per unit mass, θ is the absolute temperature, $\bar{\mathbf{Q}} = J^e (\mathbf{F}^e)^{-1} \mathbf{q}$ is the heat flux in $\bar{\mathcal{B}}$ and \mathbf{q} the heat flux in \mathcal{B} . Assume the Helmholtz free energy density in $\bar{\mathcal{B}}$ may be additively decomposed (called ‘‘energy separate’’) as

$$\bar{\rho} \psi := \bar{\rho} \psi^{\Theta^e}(J^e, \theta) + \bar{\rho} \psi^e(\dot{\mathbf{E}}^e, \theta) + \bar{\rho} \psi^p(\bar{\epsilon}_{ss}, \bar{\boldsymbol{\beta}}, \theta) + \bar{\rho} g(\theta) \quad (11)$$

where $\bar{\rho} \psi^{\Theta^e}$ is the free energy density associated with volumetric elastic deformation J^e , $\bar{\rho} \psi^e$ is the free energy density associated with isochoric elastic strain $\dot{\mathbf{E}}^e$, $\bar{\rho} \psi^p$ is the free energy density associated with the presence of dislocation defects $\bar{\epsilon}_{ss}$ and $\bar{\boldsymbol{\beta}}$, and $\bar{\rho} g$ a free energy density that can be used to define entropy, where all are functions of temperature θ . $\bar{\epsilon}_{ss}$ is the lattice deformation due to the presence of statistically-stored dislocations (SSDs), and $\bar{\boldsymbol{\beta}}$ is a strain-like internal state variable associated with the Bauschinger effect (i.e., leads to the existence of a backstress for modeling cyclic loading). The strain-like internal state variables $\bar{\epsilon}_{ss}$ and $\bar{\boldsymbol{\beta}}$ are defined in the plastically deformed configuration $\bar{\mathcal{B}}$ because their evolution equations assume a plastically deformed state. Equation (11) demonstrates the view that plastic deformation is the motion of dislocations, and the state of the material is a freeze-frame of the deformed state, which is represented by the elastic lattice deformation due to the presence of defects (dislocations) and due to external loading. We have ignored the continuum representation of geometrically necessary dislocations (GNDs) leading to a physically-motivated backstress [1–3], in order to simplify the formulation and finite element implementation. Eventually, the effect of GNDs will be included more explicitly in the model.

Substituting Eqs.(8) and (11) into Eq.(10), and using $\boldsymbol{\sigma} = (J^e)^{-1/3} \dot{\mathbf{F}}^e \bar{\mathbf{S}} (\dot{\mathbf{F}}^e)^T = \mathbf{s} + p \mathbf{1}$ ($\bar{\mathbf{S}}$ is the Second Piola Kirchhoff stress in $\bar{\mathcal{B}}$), $\mathbf{s} = \text{dev} \boldsymbol{\sigma}$, $p = \text{tr} \boldsymbol{\sigma}/3$, the Clausius-Duhem inequality in the intermediate configuration $\bar{\mathcal{B}}$ becomes

$$\begin{aligned} &\underbrace{\left(-\frac{\partial(\bar{\rho} \psi^{\Theta^e})}{\partial J^e} + p \right) j^e}_{\text{volumetric elasticity}} + \underbrace{\left(-\frac{\partial(\bar{\rho} \psi^e)}{\partial \dot{\mathbf{E}}^e} + (J^e)^{2/3} \overline{\text{Dev}} \bar{\mathbf{S}} \right) : \dot{\mathbf{E}}^e}_{\text{isochoric elasticity}} \\ &\underbrace{\left(-\left[\frac{\partial(\bar{\rho} \psi^p)}{\partial \bar{\epsilon}_{ss}} \dot{\bar{\epsilon}}_{ss} + \frac{\partial(\bar{\rho} \psi^p)}{\partial \bar{\boldsymbol{\beta}}} : \dot{\bar{\boldsymbol{\beta}}} \right] + (J^e)^{2/3} (\overline{\text{Dev}} \bar{\mathbf{S}}) : (\dot{\mathbf{C}}^e \bar{\mathbf{L}}^p) \right)}_{\text{plasticity}} + \\ &\underbrace{\left(-\frac{\partial(\bar{\rho} \psi)}{\partial \theta} - \left(\frac{\bar{\rho} \psi}{J^\theta} \right) \frac{\partial J^\theta}{\partial \theta} - \bar{\rho} \eta + 3 f^\theta J^e p \right) \dot{\theta}}_{\text{entropy}} + \underbrace{\frac{1}{\theta} \bar{\mathbf{Q}}(\bar{\nabla} \theta)}_{\text{heat}} \geq 0 \end{aligned} \quad (12)$$

where $f^\theta = (F^\theta)^{-1} \partial F^\theta / \partial \theta$, and $\overline{\text{Dev}} \bar{\mathbf{S}} := \bar{\mathbf{S}} - (\dot{\mathbf{C}}^e : \bar{\mathbf{S}}/3)(\dot{\mathbf{C}}^e)^{-1}$. Following standard thermodynamic arguments [12, 13] that \dot{J}^e , $\dot{\mathbf{E}}^e$, and $\dot{\theta}$ can vary independently, in order for Eq.(12) to be satisfied, constitutive equations for the stress and entropy are

$$p = \frac{\partial(\bar{\rho}\psi^{\Theta^e})}{\partial J^e} \quad (13)$$

$$\overline{\text{Dev}} \bar{\mathbf{S}} = \frac{1}{(J^e)^{2/3}} \frac{\partial(\bar{\rho}\psi^e)}{\partial \dot{\mathbf{E}}^e} \quad (14)$$

$$\bar{\rho}\eta = -\frac{\partial(\bar{\rho}\psi)}{\partial \theta} - \left(\frac{\bar{\rho}\psi}{J^\theta} \right) \frac{\partial J^\theta}{\partial \theta} + 3f^\theta J^e p \quad (15)$$

Defining internal stresses due to dislocation defects as

$$\bar{\kappa} := \frac{\partial(\bar{\rho}\psi^p)}{\partial \bar{\epsilon}_{ss}}, \quad \bar{\alpha} := \frac{\partial(\bar{\rho}\psi^p)}{\partial \dot{\beta}}, \quad (16)$$

the reduced dissipation inequality becomes

$$\underbrace{(J^e)^{2/3} (\overline{\text{Dev}} \bar{\mathbf{S}}) : (\dot{\mathbf{C}}^e \bar{\mathbf{L}}^p)}_{\text{plastic dissipation}} - \underbrace{\left[\bar{\kappa} \dot{\epsilon}_{ss} + \bar{\alpha} : \dot{\beta} \right]}_{\text{stored work, dislocations}} + \underbrace{\frac{1}{\theta} \bar{Q}(\bar{\nabla} \theta)}_{\text{heat}} \geq 0 \quad (17)$$

where $\bar{\kappa}$ is the internal stress due to the presence of SSDs energy conjugate to $\dot{\epsilon}_{ss}$, and $\bar{\alpha}$ is a phenomenological backstress energy conjugate to $\dot{\beta}$. Because the deviatoric stress $\overline{\text{Dev}} \bar{\mathbf{S}}$ is energy conjugate to $\dot{\mathbf{C}}^e \bar{\mathbf{L}}^p$, we use this stress in formulating the plastic evolution equations in the $\bar{\mathcal{B}}$ configuration [14]. We can account for adiabatic heating as a result of high strain rate plastic deformation in metals, but we leave this for future inclusion into the model.

Constitutive Equations

The constitutive equations involve assumptions for functional forms, based on experimental evidence, for the following physical phenomena we consider in this short paper: (i) elastic deformation, (ii) plastic deformation, and (iii) thermal expansion.

Elastic Deformation Since isochoric elastic deformation is assumed to be infinitesimal and volumetric elastic deformation could be large in the shock regime, a quadratic form of the Helmholtz free energy density is chosen only for the isochoric part. For the elastic part of the Helmholtz free energy density, the volumetric and isochoric parts are defined as

$$\begin{aligned} \bar{\rho}\psi^{\Theta^e}(J^e, \theta) &:= f^{\Theta^e}(K(\theta), J^e) \\ \implies p &= \frac{\partial f^{\Theta^e}(K(\theta), J^e)}{\partial J^e} \end{aligned} \quad (18)$$

$$\begin{aligned} \bar{\rho}\psi^e(\dot{\mathbf{E}}^e, \theta) &:= \mu(\theta) \dot{\mathbf{E}}^e : \dot{\mathbf{E}}^e \\ \implies \overline{\text{Dev}} \bar{\mathbf{S}} &= (J^e)^{-2/3} 2\mu(\theta) \dot{\mathbf{E}}^e \end{aligned} \quad (19)$$

where the temperature dependent elastic moduli are defined as

$$\begin{aligned} \mu(\theta) &:= \mu_0 \check{\mu}(\theta), \quad \check{\mu}(\theta) := (1 - m_\theta(\theta - \theta_0)/\theta_M) \\ K(\theta) &:= K_0 \check{K}(\theta), \quad \check{K}(\theta) := (1 - n_\theta(\theta - \theta_0)/\theta_M) \end{aligned}$$

where m_θ, n_θ are parameters determining the temperature dependence of the elastic moduli, θ_M is the melt temperature, μ_0 is the shear modulus at reference temperature θ_0 , and $K_0 = \lambda_0 + 2\mu_0/3$ is the bulk modulus at reference temperature. Note that $f^{\Theta^e}(K(\theta), J^e)$ can be a nonlinear function of the bulk modulus $K(\theta)$ and elastic Jacobian J^e , which results in a pressure constitutive equation for an initially undamaged metal experiencing strain rates close to or within the shock regime ($> 10^4/s$) [15]. It is possible also that the bulk modulus could be a function of J^e . We leave f^{Θ^e} undefined for the moment. An expression for p in Eq.(18) easily could be obtained from an equation of state (EOS) model, but we will not discuss this aspect further given the extensive literature on EOS models for polycrystalline metals.

Recall that for polycrystalline metals, isochoric elastic deformation is infinitesimal, and thus we choose to linearize the isochoric elastic stretch tensor as [9] $\tilde{\mathbf{V}}^e \approx \tilde{\mathbf{1}} + \tilde{\mathbf{H}}$, $\|\tilde{\mathbf{H}}\| < \varepsilon$, where $\varepsilon \ll 1$ is a small number. The implications of this assumption are now demonstrated. Recall the isochoric elastic part of the deformation gradient $\dot{\mathbf{F}}^e = \tilde{\mathbf{V}}^e \mathbf{R}^e$. Now, consider the right and left isochoric elastic Cauchy-Green tensors, respectively,

$$\begin{aligned} \dot{\mathbf{C}}^e &= (\dot{\mathbf{F}}^e)^T \dot{\mathbf{F}}^e = (\mathbf{R}^e)^T (\tilde{\mathbf{V}}^e)^T \tilde{\mathbf{V}}^e \mathbf{R}^e \\ &= \tilde{\mathbf{1}} + (\mathbf{R}^e)^T (\tilde{\mathbf{H}} + \tilde{\mathbf{H}}^T) \mathbf{R}^e \end{aligned} \quad (20)$$

$$\begin{aligned} \dot{\mathbf{b}}^e &= \dot{\mathbf{F}}^e (\dot{\mathbf{F}}^e)^T = \tilde{\mathbf{V}}^e \mathbf{R}^e (\mathbf{R}^e)^T (\tilde{\mathbf{V}}^e)^T \\ &= \tilde{\mathbf{1}} + \tilde{\mathbf{H}} + \tilde{\mathbf{H}}^T \end{aligned} \quad (21)$$

where quadratic terms $\tilde{\mathbf{H}}(\tilde{\mathbf{H}})^T$ are ignored with respect to the linear terms $\tilde{\mathbf{H}}$. Note, however, that $\tilde{\mathbf{H}} \neq \mathbf{0}$, such that the isochoric elastic strain in $\bar{\mathcal{B}}$ is

$$\dot{\mathbf{E}}^e = (\dot{\mathbf{C}}^e - \tilde{\mathbf{1}})/2 = (\mathbf{R}^e)^T (\tilde{\mathbf{H}} + \tilde{\mathbf{H}}^T) \mathbf{R}^e / 2$$

As a result, the isochoric elastic strains are infinitesimal. In mapping constitutive equations from the intermediate configuration

$\bar{\mathcal{B}}$ to the current configuration \mathcal{B} , we will use this isochoric elastic linearization. We consider volumetric elastic deformation J^e as finite, yet in \mathcal{B} we will consider also linearized volumetric elasticity to formulate a pressure equation for the case when the loading rate is less than that of the shock regime.

Plasticity and Evolution Equations The part of the free energy density accounting for elastic strain energy due to the presence of dislocations is written as

$$\bar{\rho}\psi^p(\bar{\epsilon}_{ss}, \bar{\beta}, \theta) := c_\kappa \mu(\theta) \bar{\epsilon}_{ss}^2 + c_\alpha \mu(\theta) \bar{\beta} : \bar{\beta} \quad (22)$$

which results in the stress-like internal state variables

$$\bar{\kappa} = 2c_\kappa \mu(\theta) \bar{\epsilon}_{ss}, \quad \bar{\alpha} = 2c_\alpha \mu(\theta) \bar{\beta} \quad (23)$$

where c_κ and c_α are parameters usually set equal to 1. Later, to map $\bar{\kappa}$ and $\bar{\alpha}$ to the current configuration \mathcal{B} , we will use the following relations

$$\bar{\kappa} = \sqrt{3}(J^e)^{1/3} \kappa / \|\dot{\mathbf{b}}^e\|, \quad \bar{\alpha} = (J^e)^{1/3} (\dot{\mathbf{F}}^e)^{-1} \alpha (\dot{\mathbf{F}}^e)^{-T} \quad (24)$$

where κ and α are the corresponding stress-like internal state variables in the current configuration \mathcal{B} . The mapping in Eq.(24)₁ was obtained by treating $\bar{\kappa} = \bar{\kappa} \bar{\mathbf{1}}$ as an isotropic stress in $\bar{\mathcal{B}}$, and $\kappa = \kappa \mathbf{1}$ as an isotropic stress in \mathcal{B} . Using $\kappa = (J^e)^{-1/3} \dot{\mathbf{F}}^e \bar{\kappa} (\dot{\mathbf{F}}^e)^T$ then Eq.(24)₁ results. Because $\bar{\kappa}$ and $\bar{\alpha}$ are stress-like internal state variables, they are treated as contravariant second-order tensors in terms of push-forward and pull-back operations (see Holzapfel [16]). Refer also to Marin et al. [17] for more discussion on these operations for this model.

The plastic velocity gradient in the intermediate configuration $\bar{\mathcal{B}}$ is additively decomposed into symmetric $\bar{\mathbf{D}}^p$ and skew-symmetric $\bar{\mathbf{W}}^p$ parts

$$\dot{\bar{\mathbf{C}}}^e \bar{\mathbf{L}}^p := \bar{\mathbf{D}}^p + \bar{\mathbf{W}}^p \quad (25)$$

The evolution equations for $\bar{\mathbf{D}}^p$ and $\bar{\mathbf{W}}^p$ account for thermally-activated dislocation motion and dislocation drag at high strain rates [18, 19] as well as texture effects [20] (in a future paper). The evolution equation for $\bar{\epsilon}_{ss}$ accounts for the generation and annihilation of SSDs due to standard hardening and recovery processes, while the evolution equation for $\bar{\beta}$ accounts for the generation and annihilation of dislocations of one sign (GNDs) leading to commonly known kinematic hardening.

For formulating an evolution equation for $\bar{\epsilon}_{ss}$, we relate this strain-like internal state variable to the density of SSDs $\bar{\rho}_{ss}$. Following the Taylor assumption [21], the lattice deformation due to the presence of SSDs $\bar{\epsilon}_{ss}$ can be defined as $\bar{\epsilon}_{ss} := b\sqrt{\bar{\rho}_{ss}}$, where b is the magnitude of the Burger's vector $\bar{\mathbf{b}}$ in the intermediate configuration $\bar{\mathcal{B}}$ ($b = \|\bar{\mathbf{b}}\|$). We define $\bar{\epsilon}_{ss}$ by its evolution with respect to $\dot{\bar{\rho}}_{ss}$ as

$$\dot{\bar{\epsilon}}_{ss} = \frac{b}{2} \frac{1}{\sqrt{\bar{\rho}_{ss}}} \dot{\bar{\rho}}_{ss} \quad (26)$$

Kocks & Mecking [22] and Estrin & Mecking [23] defined an evolution equation for $\bar{\rho}_{ss}$ representing thermally-activated hardening and dynamic recovery (generation and annihilation of SSDs) as

$$\dot{\bar{\rho}}_{ss} := (c_1 \sqrt{\bar{\rho}_{ss}} - c_2(\theta) \bar{\rho}_{ss}) \dot{\bar{\epsilon}}^{p,\text{eff}} \quad (27)$$

where c_1 is a constant, c_2 is a function of temperature, and $\dot{\bar{\epsilon}}^{p,\text{eff}}$ is the effective plastic strain rate in the intermediate configuration. For thermal diffusion of dislocations, static recovery is defined by Nes [24] as

$$\dot{\bar{\rho}}_{ss} := -c_3(\theta) \bar{\rho}_{ss} \sinh(c_4(\theta) \sqrt{\bar{\rho}_{ss}}) \quad (28)$$

where c_3 and c_4 are temperature dependent functions. Dynamic and static recovery mechanisms are not decoupled physical processes, but by superposing the two equations, this allows a reduction to Nes's static recovery equation (i.e., $\dot{\bar{\epsilon}}^{p,\text{eff}} = 0$) while combining the two recovery mechanisms:

$$\dot{\bar{\rho}}_{ss} := (c_1 \sqrt{\bar{\rho}_{ss}} - c_2(\theta) \bar{\rho}_{ss}) \dot{\bar{\epsilon}}^{p,\text{eff}} - c_3(\theta) \bar{\rho}_{ss} \sinh(c_4(\theta) \sqrt{\bar{\rho}_{ss}}) \quad (29)$$

Substituting Eq.(29) back into Eq.(26), and absorbing the 1/2 in the constants results in the evolution equation for the lattice deformation due to the presence of SSDs as

$$\begin{aligned} \dot{\bar{\epsilon}}_{ss} &= [H - R_d(\theta) \bar{\epsilon}_{ss}] \dot{\bar{\epsilon}}^{p,\text{eff}} - R_s(\theta) \bar{\epsilon}_{ss} \sinh(\bar{\epsilon}_{ss}) \quad (30) \\ H &= c_6 \\ R_d(\theta) &= c_5 A(Q_3, \theta) \\ R_s(\theta) &= c_7 A(Q_4, \theta) \\ A(Q_L, \theta) &= \exp[-Q_L/(R\theta)] \end{aligned}$$

where H is the hardening parameter, $R_d(\theta)$ the temperature-dependent dynamic recovery function, $R_s(\theta)$ the temperature-dependent static recovery function, $A(Q_L, \theta)$ is a standard Arrhenius temperature dependence such that as $\theta \rightarrow 0$ then $A \rightarrow 0$ and as $\theta \rightarrow \infty$ then $A \rightarrow 1$, Q_L denotes an activation energy for a given mechanism, and R is the universal gas constant. The parameters c_5 , c_6 , c_7 , Q_3 , and Q_4 will be fit to monotonic loading data. The evolution equation for $\bar{\beta}$ is defined in a traditional hardening-minus-recovery form as [8, 25]

$$\begin{aligned} \dot{\bar{\beta}} &:= h \bar{\mathbf{D}}^p - r_d(\theta) \dot{\bar{\epsilon}}^{p,\text{eff}} \sqrt{2/3} \|\bar{\beta}\| \bar{\beta} \quad (31) \\ h &= c_4 \\ r_d(\theta) &= c_3 A(Q_2, \theta) \end{aligned}$$

where h is the hardening parameter, $r_d(\theta)$ the temperature-dependent dynamic recovery function, and parameters c_3 , c_4 , and Q_2 are fit to cyclic loading experimental data. The plastic spin was determined from crystal plasticity for double planar slip as [26]

$$\bar{\mathbf{W}}^p := \lambda_g(\bar{\mathbf{A}}\bar{\mathbf{D}}^p - \bar{\mathbf{D}}^p\bar{\mathbf{A}}) \quad (32)$$

where λ_g is a geometry parameter dependent on slip system orientation, $\bar{\mathbf{A}}$ is the symmetric deviatoric structure tensor accounting for texture in $\bar{\mathcal{B}}$. This expression for the plastic spin $\bar{\mathbf{W}}^p$ has been derived by others [27], along with the evolution of $\bar{\mathbf{A}}$. For isotropic plasticity, we choose $\bar{\mathbf{A}} = \bar{\mathbf{I}}$, leading to zero plastic spin $\bar{\mathbf{W}}^p = \mathbf{0}$ in this paper. The plastic deformation rate $\bar{\mathbf{D}}^p$ is defined separately by its magnitude and direction as

$$\bar{\mathbf{D}}^p := \|\bar{\mathbf{D}}^p\| \bar{\mathbf{N}}^p \quad (33)$$

$$\bar{\mathbf{N}}^p := \text{sym} \left(\frac{\partial \bar{\Phi}^p}{\partial \text{Dev} \bar{\mathbf{S}}} \right) / \left\| \text{sym} \left(\frac{\partial \bar{\Phi}^p}{\partial \text{Dev} \bar{\mathbf{S}}} \right) \right\| \quad (34)$$

$$\bar{\Phi}^p := \sqrt{2/3} \|\bar{\mathbf{D}}^p\| := \dot{\epsilon}^{p,\text{eff}} \quad (35)$$

where $\bar{\Phi}^p$ is the plastic potential function chosen to make $\bar{\mathbf{D}}^p$ deviatoric in $\bar{\mathcal{B}}$. The flow rule (evolution of the effective plastic strain rate) accounting for transition between thermally-activated dislocation motion and dislocation drag is defined as [18, 19]

$$\dot{\epsilon}^{p,\text{eff}} := \frac{\dot{\epsilon}_1 \dot{\epsilon}_2}{\dot{\epsilon}_1 + \dot{\epsilon}_2} \quad (36)$$

where $\dot{\epsilon}_1$ is the thermally-activated effective plastic strain rate and $\dot{\epsilon}_2$ is the effective plastic strain rate for dislocation drag. The thermally-activated effective plastic strain rate $\dot{\epsilon}_1$ is defined for unified creep plasticity at low and high stresses [28] as

$$\dot{\epsilon}_1 := f(\theta) \left[\sinh \left(\left\langle \frac{\bar{\Xi}^{\text{eff}}}{\bar{\kappa} + \bar{Y}(\theta)} - 1 \right\rangle \right) \right]^{n(\theta)} \quad (37)$$

with its temperature-dependent functions defined as

$$\begin{aligned} f(\theta) &= c_2 A(Q_1, \theta) \\ \bar{Y}(\theta) &= 2\mu_0 \bar{C}_8 f^Y(\theta) \end{aligned} \quad (38)$$

$$f^Y(\theta) = \frac{m_1}{1 + m_2 \exp(-m_3/\theta)} [1 + \tanh(m_4(m_5 - \theta))] / 2 \quad (39)$$

$$n(\theta) = c_9/\theta + c_1$$

where $f(\theta)$ and $n(\theta)$ govern the rate-sensitivity of flow stress (also known as the effective relative stress $\bar{\Xi}^{\text{eff}}$ in Eq.(37)), and $\bar{Y}(\theta)$ is the quasi-static temperature-dependent initial yield strength. The parameters Q_1 , c_1 , c_2 , and c_9 are fit to rate-sensitive, temperature-dependent flow stress data, while parameters \bar{C}_8 and m_i ($i = 1, \dots, 5$) are fit to quasi-static yield strengths at various temperatures. Note that \bar{Y} has dimensions of stress

and is defined in the intermediate configuration $\bar{\mathcal{B}}$. The stress dependent function in Eq.(37) is defined as

$$\bar{\Xi}^{\text{eff}} := \sqrt{3/2} \|\bar{\Xi}\|; \quad \bar{\Xi} := \text{Dev} \bar{\mathbf{S}} - (2/3)\bar{\alpha} \quad (40)$$

where $\bar{\Xi}^{\text{eff}}$ is the effective relative stress. The effective plastic strain rate for dislocation drag [18] is defined as

$$\dot{\epsilon}_2 := \frac{1}{B} \left(\frac{\bar{\Xi}^{\text{eff}}}{\bar{\kappa} + \bar{Y}(\theta)} \right) \quad (41)$$

where B is the viscous drag parameter. An illustration of Eq.(36) and its components can be found in Fig.2. Semi-log and standard plots demonstrate the transition from thermally-activated dislocation motion to dislocation drag. Note the sharp increase in flow stress when the effective plastic strain rate enters the drag regime, which is $\approx 5.2 \times 10^7/\text{s}$ given the drag coefficient chosen. Note also that there is a transition region of $1 \times 10^7/\text{s}$ to $6 \times 10^7/\text{s}$ strain rate, through which the flow stress is governed by a transition from thermally-activated dislocation motion to dislocation-drag-dominated plastic flow. This transition region can be shifted based on the choice of the drag coefficient B . A smaller B shifts the drag regime to higher strain rates, while a larger value of B shifts the drag regime to lower strain rates.

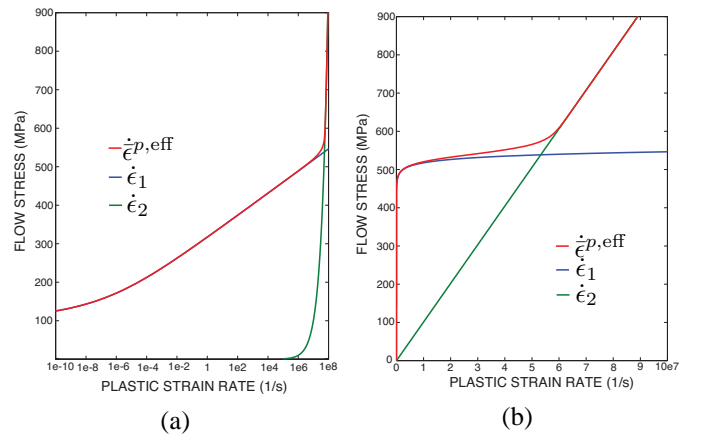


FIGURE 2. Plots of flow stress $\bar{\Xi}^{\text{eff}}$ versus effective plastic strain rate $\dot{\epsilon}^{p,\text{eff}}$ for thermally-activated dislocation motion $\dot{\epsilon}_1$ and dislocation drag $\dot{\epsilon}_2$. A drag coefficient of $B = 1 \times 10^{-7}\text{s}$ was used, along with material parameters for Tantalum in Tables 2,3. (a) semi-logarithmic, (b) standard.

Remark 1: Note that the equation for thermally-activated effective plastic strain rate and unified creep plasticity in Eq.(37), $\dot{\epsilon}_1$, can be inverted to determine a rate-dependent yield function as

$$F^Y := \bar{\Xi}^{\text{eff}} - [\bar{\kappa} + \bar{Y}(\theta)] \left(1 + \sinh^{-1} \left[(\dot{\epsilon}_1 / f(\theta))^{(1/n(\theta))} \right] \right) = 0 \quad (42)$$

where a quasi-static yield function is obtained for low plastic strain rates, i.e. when $\dot{\epsilon}_1 \approx 0$.

Deformation due to Thermal Expansion In [8], the deformation due to thermal expansion is approximated linearly as

$$\begin{aligned} F^\theta(\theta) &:= (1 + \beta(\theta)(\theta - \theta_0))^{1/3} \\ \beta(\theta) &:= \beta_0 (1 - b_\theta(\theta - \theta_0)/\theta_M) \end{aligned} \quad (43)$$

such that $J^\theta = 1 + \beta(\theta)(\theta - \theta_0)$, where β_0 is the coefficient of thermal expansion at reference temperature θ_0 . Then

$$f^\theta(\theta) := \frac{1}{F^\theta} \frac{\partial F^\theta}{\partial \theta} = \frac{\beta(\theta) + (\partial\beta(\theta)/\partial\theta)(\theta - \theta_0)}{3(1 + \beta(\theta)(\theta - \theta_0))} \quad (44)$$

Map Constitutive Equations to Current Configuration

Recall that linearized isochoric elasticity for metals means that the isochoric elastic deformation is infinitesimal, and the left and right isochoric elastic Cauchy-Green tensors are linearized in Eqs.(20) and (21). The volumetric elastic deformation, however, could be large, where $J^e = J/(J^\theta)$ for initially undamaged metals loaded in the shock regime. Note that this assumption was made in the choice of quadratic free energy function in Eq.(19), leading to linear isochoric elasticity. In the following, details of the map are outlined. In order to map the constitutive and evolution equations from $\bar{\mathcal{B}}$ to \mathcal{B} , note that $\|\bar{\mathbf{b}}^e\| \approx \sqrt{3}$ and recall the mappings

$$\begin{aligned} \overline{\text{Dev}}\bar{\mathbf{S}} &= (J^e)^{1/3} (\dot{\mathbf{F}}^e)^{-1} \mathbf{s} (\dot{\mathbf{F}}^e)^{-T} \\ \bar{\kappa} &= (J^e)^{1/3} \kappa \\ \bar{\boldsymbol{\alpha}} &= (J^e)^{1/3} (\dot{\mathbf{F}}^e)^{-1} \boldsymbol{\alpha} (\dot{\mathbf{F}}^e)^{-T} \\ \bar{\mathbf{D}}^p &= (\dot{\mathbf{F}}^e)^T \mathbf{d}^p \dot{\mathbf{F}}^e, \quad \mathbf{d}^p = \text{sym}(\boldsymbol{\ell}^p) \\ \bar{\mathbf{W}}^p &= (\dot{\mathbf{F}}^e)^T \mathbf{w}^p \dot{\mathbf{F}}^e, \quad \mathbf{w}^p = \text{skw}(\boldsymbol{\ell}^p) \\ \|\bar{\mathbf{D}}^p\| &\approx \|\mathbf{d}^p\| \end{aligned} \quad (45)$$

Substituting these expressions and expressing in rate form, the rate constitutive equations for Cauchy stress, $\boldsymbol{\sigma} = \mathbf{s} + p\mathbf{1}$, are

$$\begin{aligned} \overset{\circ}{\mathbf{s}} &:= \dot{\mathbf{s}} - \dot{\boldsymbol{\ell}}^e \mathbf{s} - \mathbf{s} (\dot{\boldsymbol{\ell}}^e)^T \\ &= (J^e)^{-1} 2\mu(\theta) \dot{\mathbf{d}}^e + \left((3f^\theta + f^{\mu\theta}) \dot{\theta} - \text{tr}(\mathbf{d}) \right) \mathbf{s} \\ \dot{p} &= \left(\frac{\partial^2 f^{\Theta e}}{\partial \theta \partial J^e} \right) \dot{\theta} + \left(\frac{\partial^2 f^{\Theta e}}{\partial J^e \partial J^e} \right) \dot{J}^e \end{aligned} \quad (46)$$

where $f^{\mu\theta} := (\partial\mu/\partial\theta)/\mu(\theta)$, and the following relations were used

$$\begin{aligned} \dot{J} &= J \text{div} \mathbf{v} \implies \dot{J}/J = \text{tr} \mathbf{d} \\ \dot{J}^e/J^e &= \dot{J}^e/J^e + \dot{J}^\theta/J^\theta \end{aligned}$$

The isochoric elastic velocity gradient $\dot{\boldsymbol{\ell}}^e$ is additively decomposed into an isochoric elastic deformation rate $\dot{\mathbf{d}}^e$ and isochoric elastic spin $\dot{\mathbf{w}}^e$ as $\dot{\boldsymbol{\ell}}^e = \dot{\mathbf{d}}^e + \dot{\mathbf{w}}^e$, where the isochoric elastic deformation rate $\dot{\mathbf{d}}^e$ is the difference between the deviatoric deformation rate $\text{dev}(\mathbf{d})$ and the plastic deformation rate \mathbf{d}^p as

$$\dot{\mathbf{d}}^e = \text{dev}(\mathbf{d}) - \mathbf{d}^p \quad (47)$$

and the isochoric elastic spin tensor $\dot{\mathbf{w}}^e$ is the difference between the total spin tensor \mathbf{w} and the plastic spin \mathbf{w}^p as $\dot{\mathbf{w}}^e = \mathbf{w} - \mathbf{w}^p$, where for isotropic plasticity $\mathbf{w}^p = \mathbf{0}$. The terms in Eq.(46) naturally appear through the mappings of Eqs.(18) and (19) to \mathcal{B} and expressing in rate form. The objective stress rate ($\overset{\circ}{\bullet}$) is called an isochoric elastic Oldroyd rate (or Truesdell rate because $\text{tr} \dot{\mathbf{d}}^e = 0$) [16], or an isochoric elastic Lie time derivative as

$$\overset{\circ}{\mathbf{s}} = \mathcal{L}_v^e(\mathbf{s}) := \dot{\mathbf{F}}^e \left[\frac{D \left((\dot{\mathbf{F}}^e)^{-1} \mathbf{s} (\dot{\mathbf{F}}^e)^{-T} \right)}{Dt} \right] (\dot{\mathbf{F}}^e)^T \quad (48)$$

Because isochoric elastic deformations are infinitesimal for metals, we can assume that $\|\mathbf{s}\| \ll \mu(\theta)$, and we ignore the $\dot{\mathbf{d}}^e \mathbf{s}$ terms on the left-hand-side with respect to the $\mu(\theta) \dot{\mathbf{d}}^e$ term on the right-hand-side of Eq.(46) such that

$$\overset{\nabla}{\mathbf{s}} := \dot{\mathbf{s}} - \dot{\mathbf{w}}^e \mathbf{s} + \mathbf{s} \dot{\mathbf{w}}^e \quad (49)$$

This stress rate can be viewed as an elastic Jaumann-Zaremba rate and is used in place of the isochoric elastic Oldroyd rate for Cauchy stress in Eq.(46)₁. The rate evolution equations for the internal stress variables κ and $\boldsymbol{\alpha}$ are

$$\begin{aligned} \dot{\kappa} &= f^{\mu\theta J} \kappa + (c_\kappa \mu^e H - R_d(\theta) \kappa) \dot{\epsilon}^{p,\text{eff}} - R_s(\theta) \kappa \sinh(\kappa/(c_\kappa \mu^e)) \\ \overset{\circ}{\boldsymbol{\alpha}} &:= \dot{\boldsymbol{\alpha}} - \dot{\boldsymbol{\ell}}^e \boldsymbol{\alpha} - \boldsymbol{\alpha} (\dot{\boldsymbol{\ell}}^e)^T \\ &= f^{\mu\theta J} \boldsymbol{\alpha} + c_\alpha \mu^e h \mathbf{d}^p - \sqrt{2/3} [r_d(\theta) \dot{\epsilon}^{p,\text{eff}} / (c_\alpha \mu^e)] \|\boldsymbol{\alpha}\| \boldsymbol{\alpha} \end{aligned}$$

where

$$\begin{aligned} f^{\mu\theta J} &:= \left(f^{\mu\theta} \dot{\theta} - (\dot{J}/J - \dot{J}^\theta/J^\theta) / 3 \right) \\ \mu^e &:= (J^e)^{-1/3} 2\mu_0 \check{\mu}(\theta) \end{aligned} \quad (50)$$

and $\dot{\epsilon}^{p,\text{eff}} \approx \dot{\epsilon}^{p,\text{eff}}$, except that all variables are evaluated in the current configuration in $\dot{\epsilon}^{p,\text{eff}}$. When writing the plastic flow rule in the current configuration, the following mappings are needed from $\bar{\mathcal{B}}$ to \mathcal{B}

$$\bar{\Xi}^{\text{eff}} = \sqrt{3/2} J^e \|\boldsymbol{\xi}\|, \quad \boldsymbol{\xi} = \mathbf{s} - (2/3)(J^e)^{-2/3} \boldsymbol{\alpha} \quad (51)$$

With the additional assumption that volumetric elastic deformation is infinitesimal (and thus linearized) for metals loaded at strain rates less than the shock regime ($< 10^4$ /s), the elastic Jacobian may be approximated as $J^e \approx 1 + \epsilon_v^e$, where the volumetric elastic strain ϵ_v^e is small relative to 1, such that $|\epsilon_v^e| < \epsilon$,

where $\varepsilon \ll 1$ is a small number. Then the volumetric elastic strain rate becomes

$$\dot{\epsilon}_v^e \approx \dot{J}^e / J^e = \text{tr} \mathbf{d} - \dot{J}^\theta / J^\theta \quad (52)$$

For linear volumetric elasticity, we choose the volumetric elastic part of the Helmholtz free energy density as

$$\bar{p}\psi^{\Theta^e} := K(\theta)(\epsilon_v^e)^2/2 \implies p = K(\theta)\epsilon_v^e \quad (53)$$

The resulting equations are summarized in Box 1.

Box 1. Summary of evolution equations for linearized volumetric and isochoric elasticity in \mathcal{B} .

$$\begin{aligned} \overset{\nabla}{\mathbf{s}} &= 2\mu(\theta)\overset{\nabla}{\mathbf{d}}^e + \left((3f^\theta + f^{\mu\theta})\dot{\theta} - \text{tr}(\mathbf{d}) \right) \mathbf{s} \\ \dot{p} &= (f^{K\theta}\dot{\theta})p + K(\theta)\dot{\epsilon}_v^e, \quad f^{K\theta} = (\partial K/\partial\theta)/K(\theta) \\ \dot{\epsilon}_1 &= f(\theta) \left[\sinh \left(\left\langle \frac{\xi^{\text{eff}}}{(\kappa + y(\theta))} - 1 \right\rangle \right) \right]^{n(\theta)} \\ \dot{\epsilon}_2 &= \frac{1}{B} \frac{\xi^{\text{eff}}}{(\kappa + y(\theta))}, \quad \xi^{\text{eff}} = \sqrt{3/2} \|\xi\| \\ \xi &= \mathbf{s} - (2/3)\alpha \\ \dot{\kappa} &= f^{\mu\theta J} \kappa + (c_\kappa 2\mu(\theta)H - R_d(\theta)\kappa) \dot{\epsilon}^{p,\text{eff}} \\ &\quad - R_s(\theta)\kappa \sinh(c_{10}\kappa/(c_\kappa 2\mu(\theta))) \\ \dot{\alpha} &= f^{\mu\theta J} \alpha + c_\alpha 2\mu(\theta)h \mathbf{d}^p \\ &\quad - \sqrt{2/3} [r_d(\theta)\dot{\epsilon}^{p,\text{eff}}/(c_\alpha 2\mu(\theta))] \|\alpha\| \alpha \\ f^{\mu\theta J} &= f^{\mu\theta}\dot{\theta} - \dot{\epsilon}_v^e/3 \end{aligned}$$

Dimensionless Form and Plasticity Parameter Fitting

Frost & Ashby [29] recognized that the stress-strain response of polycrystalline solids with similar lattice structure and bonding (e.g., bcc metals), when normalized with appropriate normalizing parameters, collapsed to a narrow band of curves. They coined the phrase “isomechanical groups” to describe these materials and their respective similar mechanical behavior when their evolution equations are normalized. From a practical engineering perspective, taking advantage of such behavior is very appealing when given experimental data at few temperatures and strain-rates used to characterize the mechanical response of a polycrystalline metal. We will demonstrate that dimensionless parameters fit to data of one bcc metal (Tantalum) can be used to approximate the response of another bcc metal (Tungsten). The expectation is that by using such parameters fit for one metal to approximate the behavior of another metal in the same isomechanical group, that extrapolating mechanical response beyond available experimental data will be better informed than if parameters are fit only to the limited data set. The normalizing parameters are:

Burgers vector (**length**) b

melt **temperature** θ_M

$2\times$ shear modulus (**dislocation internal variables**) $2\mu(\dot{\theta})$

characteristic **time** $\tau = b^2/d_M$

where b is the Burgers vector at reference temperature θ_0 , $d_M = d_0 \exp[-Q_d/(R\theta_M)]$ is the diffusivity at melt [29], d_0 is the diffusivity prefactor, and Q_d the diffusivity activation energy. The dimensionless variables, parameters, and rates are summarized in Table 1.

time	$\check{t} = t/\tau$
differential time	$d\check{t} = dt/\tau$
temperature	$\check{\theta} = \theta/\theta_M$
mass density	$\check{\rho}_0 = \rho_0 b^2 / (2\mu(\check{\theta})\tau^2)$
coefficient of thermal expansion	$\check{\beta}(\check{\theta}) = \theta_M \beta(\check{\theta})$
specific heat	$\check{c}_v(\check{\theta}) = c_v \tau^2 \theta_M / b^2$
free energy per unit mass	$\check{\psi} = \psi \tau^2 / b^2$
time derivative	$(\dot{\bullet}) = \tau(\dot{\bullet})$
rate	$(\check{\bullet}) = \tau(\bullet)$
deviatoric stress	$\check{\mathbf{s}} = \mathbf{s} / (2\mu(\check{\theta}))$
pressure	$\check{p} = p / K(\check{\theta})$
internal backstress	$\check{\alpha} = \alpha / (2\mu(\check{\theta}))$
isotropic internal stress	$\check{\kappa} = \kappa / (2\mu(\check{\theta}))$

TABLE 1. Dimensionless variables.

One-dimensional Uniaxial Stress Form of Model

For fitting plasticity parameters and testing the model formulation, a one-dimensional uniaxial stress condition is assumed, for which the plastic spin $\mathbf{w}^p = \mathbf{0}$ and spin $\mathbf{w} = \mathbf{0}$. The formulation is carried out for the dimensionless form of the model. Given an axial stress $\check{\sigma}$, axial strain rate $\check{\epsilon}$, axial elastic strain rate $\check{\epsilon}^e$, axial plastic strain rate $\check{\epsilon}^p$, and axial backstress $\check{\alpha}$, the deformation rate and stress tensors are written as

$$\begin{aligned} \check{\mathbf{d}}^e &= \check{\epsilon}^e \begin{bmatrix} 1 & 0 & 0 \\ 0 & -\nu & 0 \\ 0 & 0 & -\nu \end{bmatrix}, \quad \check{\mathbf{d}}^p = \check{\epsilon}^p \begin{bmatrix} 1 & 0 & 0 \\ 0 & -1/2 & 0 \\ 0 & 0 & -1/2 \end{bmatrix} \\ \check{\boldsymbol{\sigma}} &= \begin{bmatrix} \check{\sigma} & 0 & 0 \\ 0 & 0 & 0 \\ 0 & 0 & 0 \end{bmatrix}, \quad \check{\mathbf{s}} = (\check{\sigma}/3) \begin{bmatrix} 2 & 0 & 0 \\ 0 & -1 & 0 \\ 0 & 0 & -1 \end{bmatrix} \\ \check{\alpha} &= \check{\alpha} \begin{bmatrix} 1 & 0 & 0 \\ 0 & -1/2 & 0 \\ 0 & 0 & -1/2 \end{bmatrix} \\ \check{\xi} &= \check{\mathbf{s}} - (2/3)\check{\alpha} = (\check{\sigma} - \check{\alpha})/3 \begin{bmatrix} 2 & 0 & 0 \\ 0 & -1 & 0 \\ 0 & 0 & -1 \end{bmatrix} \end{aligned}$$

We evaluate some of the kinematic variables using the uniaxial stress assumption, such that

$$\check{\mathbf{d}} = \check{\mathbf{d}}^e + \check{\mathbf{d}}^p + f^{\check{\theta}} \check{\theta} \mathbf{1} \quad (54)$$

$$\text{tr} \check{\mathbf{d}} = (1 - 2\nu) \check{\epsilon}^e + 3f^{\check{\theta}} \check{\theta} \quad (55)$$

$$\check{\mathbf{d}}^e = \text{dev}(\check{\mathbf{d}}) - \check{\mathbf{d}}^p = (1 + \nu) \check{\epsilon}^e / 3 \begin{bmatrix} 2 & 0 & 0 \\ 0 & -1 & 0 \\ 0 & 0 & -1 \end{bmatrix} \quad (56)$$

For the 1D case, we must normalize the pressure p the same as the deviatoric stress s in order to add them together to get the total stress. In addition, we assume the temperature dependence of the shear and bulk moduli are the same, i.e. $m_\theta = n_\theta$. Then,

$$\begin{aligned} \check{p} &= \frac{K(\check{\theta})}{2\mu(\check{\theta})} \check{\epsilon}_v^e = \frac{1 + \nu}{3(1 - 2\nu)} \check{\epsilon}_v^e \\ \check{p} &= \frac{1 + \nu}{3(1 - 2\nu)} \check{\epsilon}_v^e, \quad \check{\epsilon}_v^e = \text{tr} \check{\mathbf{d}}^e = (1 - 2\nu) \check{\epsilon}^e \\ &\implies \check{p} = (1 + \nu) \check{\epsilon}^e / 3 \end{aligned} \quad (57)$$

Note that $\check{p} = \check{\sigma} / 3$. We then obtain the deviatoric stress rate

$$\check{\mathbf{s}} = \left[(1 + \nu) \check{\epsilon}^e / 3 - (1 - 2\nu) \check{\epsilon}^e (\check{\sigma} / 3) \right] \begin{bmatrix} 2 & 0 & 0 \\ 0 & -1 & 0 \\ 0 & 0 & -1 \end{bmatrix} \quad (58)$$

The total stress is $\check{\boldsymbol{\sigma}} = \check{\mathbf{s}} + \check{p} \mathbf{1}$, leading to

$$\begin{aligned} \check{\boldsymbol{\sigma}} \begin{bmatrix} 1 & 0 & 0 \\ 0 & 0 & 0 \\ 0 & 0 & 0 \end{bmatrix} &= (1 + \nu) \check{\epsilon}^e \begin{bmatrix} 1 & 0 & 0 \\ 0 & 0 & 0 \\ 0 & 0 & 0 \end{bmatrix} \\ &- [(1 - 2\nu) \check{\epsilon}^e \check{\sigma} / 3] \begin{bmatrix} 2 & 0 & 0 \\ 0 & -1 & 0 \\ 0 & 0 & -1 \end{bmatrix} \end{aligned} \quad (59)$$

As for the three-dimensional equations, the elastic strain power term $\check{\epsilon}^e \check{\boldsymbol{\sigma}}$ can be shown to be small relative to the elastic rate term $\check{\epsilon}^e$ in Eq.(59). Similarly, we make this argument for ignoring the terms $\check{\epsilon}^e \check{\boldsymbol{\alpha}}$ and $\check{\epsilon}^e \check{\kappa}$ in the evolution equations for the internal stresses. Since $\|\check{\boldsymbol{\alpha}}\| = \sqrt{3/2} |\check{\alpha}|$ and $\|\check{\mathbf{d}}^p\| = \sqrt{3/2} |\check{\epsilon}^p|$, the rest of the evolution equations are determined. A summary of equations are listed in Box 2. We will solve these equations to fit plasticity parameters next.

Box 2. Summary of dimensionless evolution equations for linearized volumetric and isochoric elasticity in \mathcal{B} under uniaxial stress conditions.

$$\begin{aligned} \check{\sigma} &= (1 + \nu) \check{\epsilon}^e \\ \check{\epsilon}^e &= \check{\epsilon} - \check{\epsilon}^p - f^{\check{\theta}} \check{\theta} \\ \check{\epsilon}^p &= \frac{\check{\epsilon}_1 \check{\epsilon}_2}{\check{\epsilon}_1 + \check{\epsilon}_2} \\ \check{\epsilon}_1 &= f^{\check{\theta}} \left[\sinh \left(\left\langle \frac{\check{\xi}^{\text{eff}}}{\check{\kappa} + \check{y}(\check{\theta})} - 1 \right\rangle \right) \right]^{n(\check{\theta})} \\ \check{\epsilon}_2 &= \frac{1}{\check{B}} \frac{\check{\xi}^{\text{eff}}}{\check{\kappa} + \check{y}(\check{\theta})} \\ \check{\boldsymbol{\alpha}} &= \left(c_\alpha h - \frac{r_d(\check{\theta})}{c_\alpha} \text{sign}(\check{\epsilon}^p) |\check{\boldsymbol{\alpha}}| \right) \check{\epsilon}^p \\ \check{\kappa} &= [c_\kappa H - R_d(\check{\theta}) \check{\kappa}] |\check{\epsilon}^p| - \check{R}_s(\check{\theta}) \check{\kappa} \sinh \left(\frac{\check{\kappa}}{c_\kappa} \right) \\ \check{\xi}^{\text{eff}} &= |\check{\sigma} - \check{\boldsymbol{\alpha}}| \end{aligned}$$

Plasticity Parameter Fitting The process of plasticity parameter fitting involves three steps: (1) obtain the physical constants for your metal of interest in [29] (e.g., for Tantalum and Tungsten in Table 2), (2) fit parameters m_i in Eq.(39) for quasi-static yield data, and (3) fit the remaining parameters to isothermal, uniaxial stress data for various temperatures and strain rates.

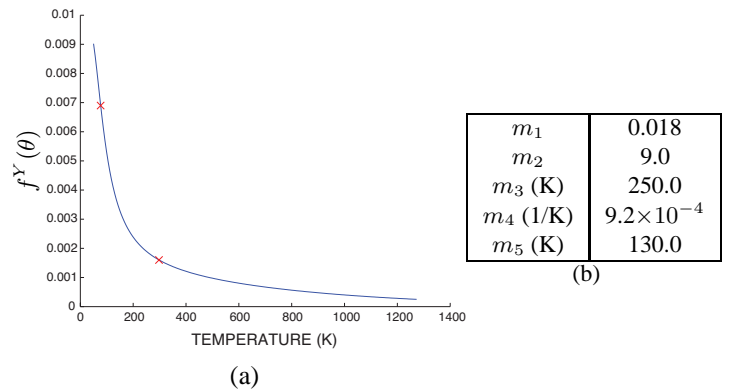


FIGURE 3. (a) Plot of fit of $f^Y(\theta)$ in Eq.(39) to quasi-static yield data for Tantalum [30]. (b) Temperature dependent yield parameters fit to quasi-static yield stress data for Tantalum.

Tantalum: The fit to quasi-static yield stress for Tantalum is shown in Fig.3. Quasi-static yield stress is known only for

R (J/(K mol))	8.314	R (J/(K mol))	8.314
b (m)	2.86×10^{-10}	b (m)	2.74×10^{-10}
θ_M (K)	3271	θ_M (K)	3683
d_0 (m ² /s)	1.2×10^{-5}	d_0 (m ² /s)	5.6×10^{-4}
Q_d (J/mol)	4.13×10^5	Q_d (J/mol)	5.85×10^5
E_0 (Pa)	16.8×10^{10}	E_0 (Pa)	41.0×10^{10}
ν_0	0.34	ν_0	0.28
ρ (kg/m ³)	16.6×10^3	ρ (kg/m ³)	19.3×10^3
c_v (J/(K kg))	142.0	c_v (J/(K kg))	138.0
B (s)	0	B (s)	0
m_θ	0.42	m_θ	0.38
n_θ	0.42	n_θ	0.38
θ_0 (K)	298	θ_0 (K)	298
β_0 (1/K)	6.5×10^{-6}	β_0 (1/K)	4.5×10^{-6}
κ_0 (Pa)	0	κ_0 (Pa)	0
α_0 (Pa)	0	α_0 (Pa)	0
c_α	1	c_α	1
c_κ	1	c_κ	1

TABLE 2. Summary of physical, *pre-determined* constants for (a) Tantalum and (b) Tungsten.

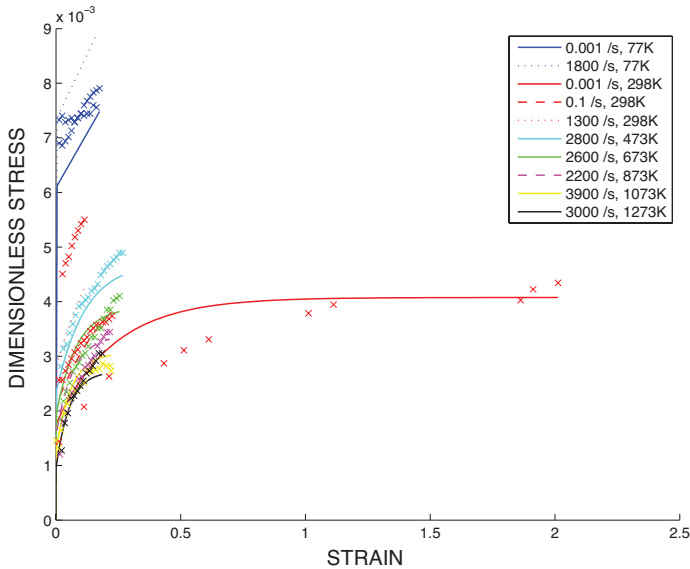


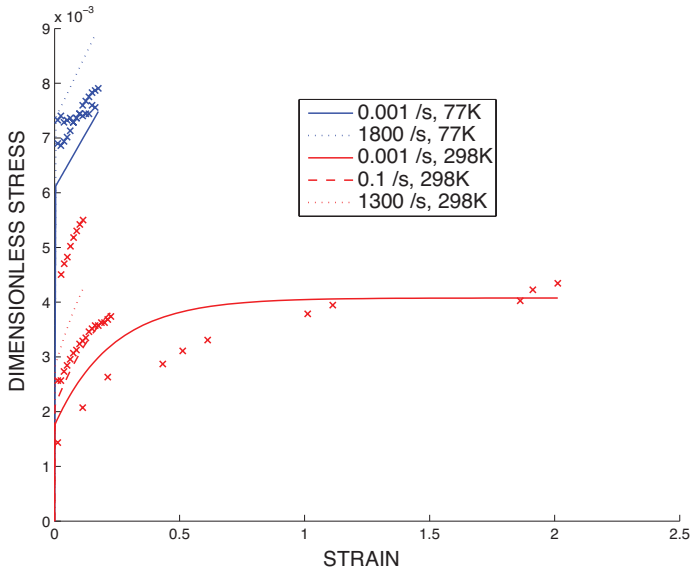
FIGURE 4. Resulting fit of Tantalum uniaxial compression data [30].

temperatures 77K and 298K [30]. This involves fitting $f^Y(\theta)$ in Eq.(38) to the normalized yield stress $y(\theta)/[2\mu(\theta)]$ at known temperatures (i.e., 77K and 298K) for an undamaged current configuration (or current configuration with known porosity) and assuming $c_8 = 1$. The resulting parameters are shown in Fig.3(b). Figures 4 and 5 show the dimensionless fit for various temperatures and strain rates for Tantalum isothermal, uniaxial stress data in [30]. The resulting fitting parameters are shown in Table 3(a). The fit bounds the data, but does a poor job of fitting the 298K, 1300/s strain rate data; and a less than satisfactory job of fitting the 77K data (low and high strain rates).

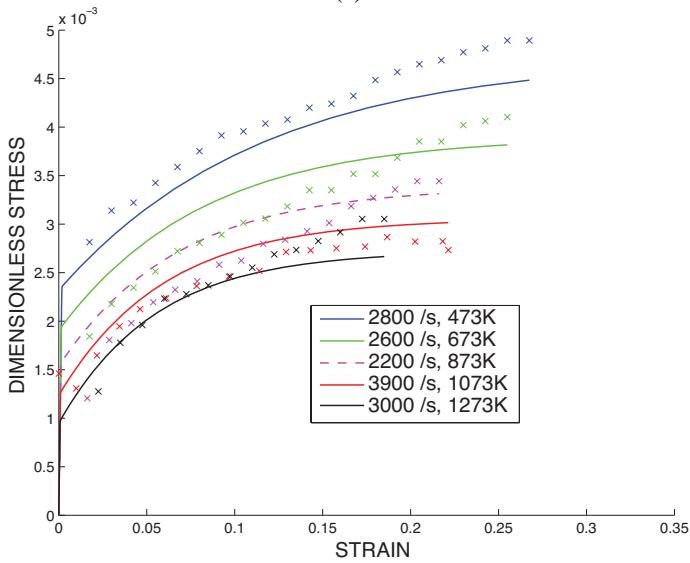
Tungsten: Given the physical constants in Table 2(b) for Tungsten and the dimensionless fitting parameters for Tantalum in Table 3(a) (also a bcc metal, and specifically a refractory metal of the same isomechanical group [29]), we expect an initial representation of the Tungsten response to be reasonable. Figure 6 shows an application of the dimensionless parameters for Tantalum to the Tungsten data, using the Tungsten physical constants, and shows that the initial fit is in the range of the data. The fit to quasi-static yield stress for Tungsten is shown in Fig.7(a). Quasi-static yield stress is known only for temperatures 77K and 298K [31]. The resulting parameters are shown in Fig.7(b). Figure 8 shows the fit to Tungsten uniaxial compression data with the dimensionless parameters shown in Table 3(b). Clearly, this re-calibration of Tungsten dimensionless fitting parameters does a better job fitting the data in Fig.8 than using the dimensionless Tantalum fitting parameters in Table 3(a), but the dimensionless Tantalum fitting parameters at the very least provide a good initial guess to the fit.

CONCLUSIONS

The paper presented a finite strain, rate and temperature dependent elasto-plastic constitutive model for polycrystalline metals. A multiplicative decomposition of the deformation gradient into elastic, plastic, and thermal parts is employed, along with a volumetric-isochoric split of the elastic deformation gradient \mathbf{F}^e . Isochoric elastic deformations in metals are assumed infinitesimal, whereas volumetric elastic deformation for initially nearly undamaged metals can be large at high strain rates. Generation and annihilation of statistically-stored dislocations (SSDs) is accounted for, along with dislocation drag at high strain rates. A dimensionless form of the model is presented using the approach of isomechanical groups by Frost and Ashby, demonstrating a fit of dimensionless plastic parameters for Tantalum, a body centered cubic (bcc) lattice structure refractory metal, and applying them to Tungsten, another bcc refractory metal. The initial fit of Tungsten data using Tantalum dimensionless plastic parameters provides a reasonable initial guess for the fit, that is easily refined, as demonstrated in the paper. Future work involves extending the model to include isotropic damage, texture effects, adiabatic heating, and three-dimensional numerical examples.



(a)



(b)

FIGURE 5. Resulting fit of Tantalum uniaxial compression data, separated into (a) low and (b) high temperature ranges for better viewing.

ACKNOWLEDGMENT

The authors acknowledge earlier financial support for the model development through a Memorandum of Understanding (MOU) between the U.S. Department of Defense (DOD) and Department of Energy (DOE), under the direction of Bob Garrett of the U.S. Navy and Gene Hertel of Sandia National Laboratories. The authors acknowledge earlier efforts by David Patillo in developing an algorithm for fitting the dimensionless material parameters.

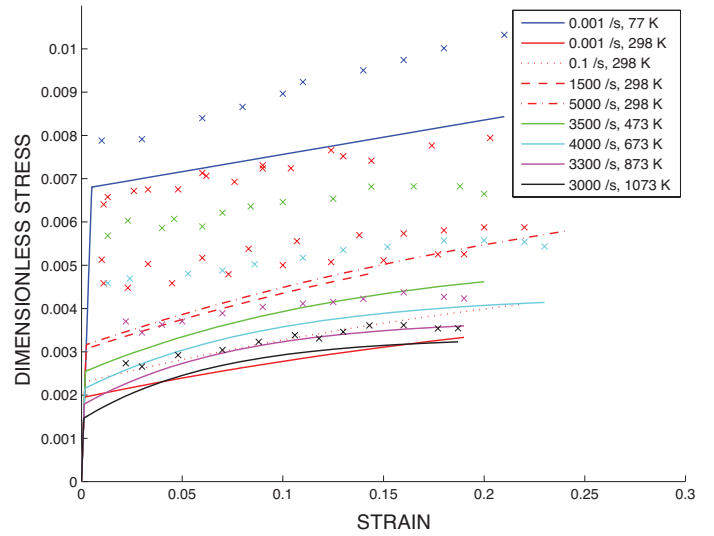
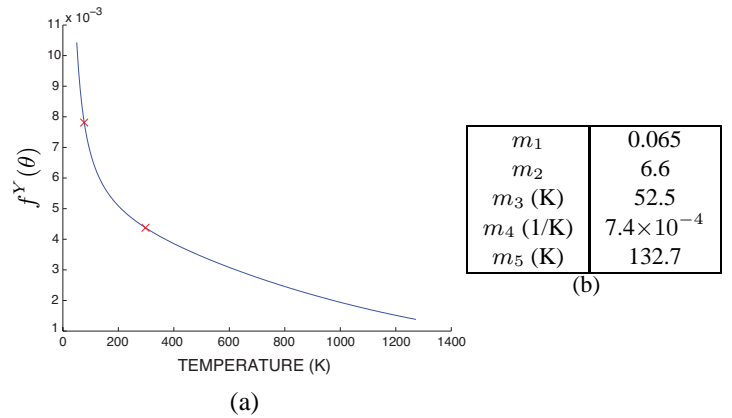


FIGURE 6. Applying dimensionless fitting parameters for Tantalum to Tungsten uniaxial compression data.



(a)

FIGURE 7. (a) Plot of fit of $f^Y(\theta)$ in Eq.(39) to quasi-static yield data for Tungsten. (b) Temperature dependent yield parameters fit to quasi-static yield stress data for Tungsten.

REFERENCES

- [1] D.J. Bammann, 2001. "A model of crystal plasticity containing a natural length scale". *Mat. Sci. Engr.*, **A309-310**, pp. 406-410.
- [2] R.A. Regueiro and D.J. Bammann and E.B. Marin and K. Garikipati, 2002. "A nonlocal phenomenological anisotropic finite deformation plasticity model accounting for dislocation defects". *J. Eng. Mater. Technol.*, **124**, pp. 380-387.
- [3] Clayton, J., McDowell, D., and Bammann, D., 2006. "Modeling dislocations and disclinations with finite micropolar elastoplasticity". *Int. J. Plast.*, **22**(2), pp. 210 -

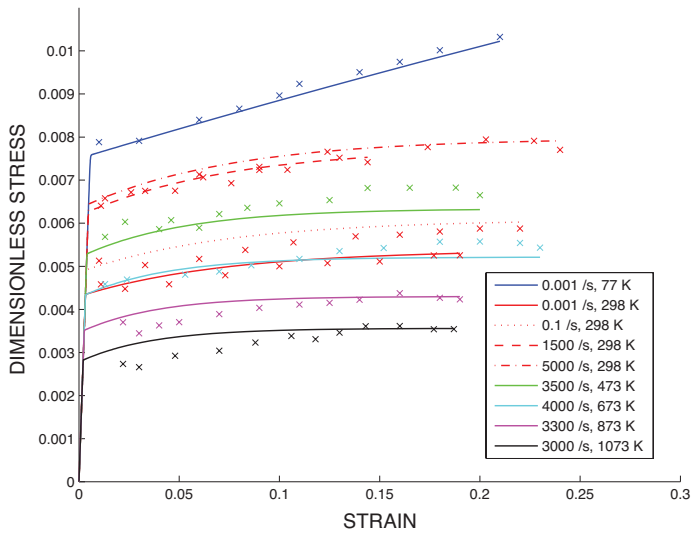


FIGURE 8. Resulting fit of Tungsten uniaxial compression data [31].

c_1	1.73	c_1	14.1
\check{c}_2	1.4×10^{-14}	\check{c}_2	3.4×10^{-12}
c_3	0	c_3	0
c_4	0	c_4	0
c_5	28.7	c_5	36.8
c_6	3.87×10^{-3}	c_6	7.1×10^{-3}
\check{c}_7	5.4×10^{-6}	\check{c}_7	5.4×10^{-6}
c_8	0.43	c_8	0.5
\check{c}_9	0.64	\check{c}_9	7.8×10^{-3}
\check{Q}_1	1.4×10^{-5}	\check{Q}_1	3.0×10^{-4}
\check{Q}_2	0	\check{Q}_2	0
\check{Q}_3	0.17	\check{Q}_3	0.08
\check{Q}_4	9.88	\check{Q}_4	9.88

TABLE 3. Summary of dimensionless fitting parameters for (a) Tantalum and (b) Tungsten.

256.

- [4] Klein, P., McFadden, S., Bammann, D., Hammi, Y., Foulk, J., and Antoun, B., 2003. A mechanism-based approach to modeling ductile fracture. SAND2003-8804, Sandia National Laboratories.
- [5] Lee, E., 1969. "Elastic-plastic deformation at finite strains". *J. App. Mech.*, **36**, pp. 1–6.
- [6] Davison, L., Stevens, A., and Kipp, M., 1977. "Theory

of spall damage accumulation in ductile metals". *J. Mech. Phys. Solids*, **25**, pp. 11–28.

- [7] Bammann, D., and Aifantis, E., 1989. "A damage model for ductile metals". *Nucl. Eng. Des.*, **116**, pp. 355–362.
- [8] Bammann, D., Chiesa, M., and Johnson, G., 1996. "Modeling large deformation and failure in manufacturing processes". In *Theoretical and Applied Mechanics*, T. Tatsuji, E. Watanabe, and T. Kambe, eds. Elsevier Science, pp. 359–376.
- [9] Bammann, D., and Johnson, G., 1987. "On the kinematics of finite deformation plasticity". *Acta Mech.*, **70**, pp. 1–13.
- [10] Flory, P., 1961. "Thermodynamic relations for high elastic materials". *Trans. Faraday Soc.*, **57**, pp. 829–838.
- [11] Simo, J., Taylor, R., and Pister, K., 1985. "Variational and projection methods for the volume constraint in finite deformation elasto-plasticity". *Comp. Meth. App. Mech. Engr.*, **51**, pp. 177–208.
- [12] Coleman, B. D., and Noll, W., 1963. "The thermodynamics of elastic materials with heat conduction and viscosity". *Arch. Ration. Mech. Anal.*, **13**, pp. 167–178.
- [13] Coleman, B. D., and Gurtin, M. E., 1967. "Thermodynamics with internal state variables". *J. Chem. Phys.*, **47**, pp. 597–613.
- [14] Mandel, J., 1974. "Thermodynamics and plasticity". In *Foundations of Continuum Thermodynamics*, J. D. et al., ed. Macmillan, New York, pp. 283–304.
- [15] Davison, L., and Graham, R., 1979. "Shock compression of solids". *Phys. Report*, **55(4)**, pp. 255–379.
- [16] Holzapfel, G. A., 2000. *Nonlinear Solid Mechanics: A Continuum Approach for Engineering*. John Wiley & Sons.
- [17] Marin, E., Bammann, D., Regueiro, R., and Johnson, G., 2005. On the Formulation, Parameter Identification and Numerical Integration of the EMMI Model: Plasticity and Isotropic Damage. SAND2004, Sandia National Laboratories.
- [18] Klahn, D., Mukherjee, A., and Dorn, J., 1970. "Strain-rate effects". In *Second International Conference on the Strength of Metals and Alloys*, American Society for Metals: Metals Park, OH, pp. 951–982.
- [19] Follansbee, P., 1988. "The rate dependence of structure evolution in copper and its influence on the stress-strain behavior at very high strain rates". In *Impact Loading and Dynamic Behaviour of Materials*, C. Chiem, H.-D. Kunze, and L. Meyer, eds., Verlag, Germany, pp. 315–322.
- [20] Kocks, U., Tome, C., and Wenk, H.-R., 1998. *Texture and Anisotropy*. Cambridge University Press.
- [21] Taylor, G., 1934. "The mechanism of plastic deformation of crystals. Part I. Theoretical". *Proc. R. Soc. Lond. A, Math. Phys. Eng. Sci.*, **A145**, pp. 362–387.
- [22] Kocks, U., and Mecking, H., 1979. "A mechanism for static and dynamic recovery". In *Strength of Metals and Alloys*, P. Haasen, V. Gerold, and G. Kostorz, eds. Pergamon Press,

- pp. 345–350.
- [23] Estrin, Y., and Mecking, H., 1984. “A unified phenomenological description of work hardening and creep based on one-parameter models”. *Acta Metall.*, **32**, pp. 57–70.
 - [24] Nes, E., 1995. “Recovery revisited”. *Acta Metall. Mater.*, **43**, pp. 2189–2207.
 - [25] D.J. Bammann, 1990. “Modeling the temperature and strain rate dependent large deformation of metals”. *App. Mech. Rev.*, **43**, pp. S312–S319.
 - [26] Prantil, V., Jenkins, J., and Dawson, P., 1993. “An analysis of texture and plastic spin for planar polycrystals”. *J. Mech. Phys. Solids*, **41**, pp. 1357–1382.
 - [27] Dafalias, Y., 2000. “Orientational evolution of plastic orthotropy in sheet metals”. *J. Mech. Phys. Solids*, **48**, pp. 2231–2255.
 - [28] Garofalo, F., Richmond, C., Domis, W., and von Gemmingen, F., 1963. “Strain-time, rate-stress and rate-temperature relations during large deformations in creep”. In Joint International Conference on Creep, Vol. 1, pp. 31–39.
 - [29] Frost, H., and Ashby, M., 1982. *Deformation-Mechanism Maps*. Pergamon Press.
 - [30] Chen, S., and III, G. G., 1996. “Constitutive behavior of tantalum and tantalum-tungsten alloys”. *Metall. Mat. Trans. A Phys. Metall. Mat. Sci.*, **27A**, pp. 2994–3006.
 - [31] Chen, S., and III, G. G., 1994. “Constitutive behavior of Tungsten and Tantalum: Experiments and modeling”. In *Tungsten and Refractory Metals 2*, A. Bose and R. Dowling, eds., Metal Powder Industries Federation, pp. 489–498.